A one-dimensional theoretical prediction of the effect of reduced endplate permeability on the mechanics of the intervertebral disc.

Riches PE[1], McNally DS[2].

[1]Department of Applied Physiology, University of Strathclyde, UK. [2]School of Mechanical, Materials, Manufacturing Engineering and Management, University of Nottingham, UK.

Address for correspondence:

Dr. Philip Riches

Department of Applied Physiology

Faculty of Science

University of Strathclyde

76 Southbrae Drive

Glasgow

G13 1PP

Scotland

philip.riches@strath.ac.uk

A one-dimensional theoretical prediction of the effect of reduced endplate permeability on the mechanics of the intervertebral disc.

Riches PE[1], McNally DS[2].

[1]SIBS, University of Strathclyde, [2]School of Mechanical, Materials, Manufacturing Engineering and Management, University of Nottingham.

Abstract

The permeability of the cartilage end-plate (CEP) may play an important role in intervertebral disc (IVD) degeneration by controlling the convective and diffusive transport of metabolites into the nucleus pulposus. A one-dimensional poroelastic model was used to predict the effect of a CEP of lower permeability than the disc tissue on the convective transfer into and out of the IVD. With decreasing CEP permeability, associated with degeneration, the model predicted that the change in disc height with time became more linear; the disc could not rehydrate as quickly; and internal fluid movement was slowed. This study has shown that CEP permeability will only markedly have an effect on fluid movement, and hence convective nutrition, if the permeability of the CEP is reduced to less than that of the disc tissue.

Key words

intervertebral disc; poroelastic; endplate sclerosis.

Notation

k	hydraulic permeability of the intevertebral disc tissue
n	the exponent of the power law relating strain and porosity
t	time
u	fluid displacement
x	spatial variable
H_A	aggregate modulus
P	Pore pressure of fluid in tissue
U	solid displacement
ϕ	porosity
π	osmotic pressure in the tissue
σ_a	applied stress at the boundary

1 Introduction

The cartilage end-plate (CEP) is the structural unit, situated between the intervertebral disc (IVD) and the vertebral body, consisting of hyaline cartilage of approximately 0.6mm in thickness **[1]**. The CEP is important for the mechanical functioning of the spine: under high compressive loads the CEP bulges into the vertebral bodies **[2,3]** and since the 'normal' CEP is porous, it provides one pathway via which metabolites can enter the disc, the other being through the outer annulus fibrosus **[4]**. Whilst the main mechanism for transport of small solutes, such as oxygen and glucose, is diffusion, convective transport of large enzymes and hormones may be of some importance in maintaining a healthy disc **[5]**. However, with increasing age and in some diseased states, such as scoliosis, the CEP can decrease in

permeability with calcification, hindering the transport of both large and small solutes **[6]**. This phenomenon has been previously associated with IVD degeneration **[4]** and recent empirical evidence has shown a correlation between endplate degeneration and disc degeneration **[7]**.

Since it has been shown that the axial CEP bulge is comparable in magnitude to the compression of the whole motion segment **[2]**, the height of the nucleus pulposus (NP) of the disc is similar immediately before and immediately after application of a load (Figure 1). On continued application of the load, the subsequent loss of fluid from the NP has been calculated to predominantly flow through the CEP rather than the annular route **[8]**. As a consequence of the former experimental finding and the latter theoretical result, it follows that the time-dependent mechanics of the central portion of the NP may be modeled as spatially one-dimensional **[9]**. Moreover, due to the relatively large distance from the exterior AF to the NP, the CEP nutrition route is vital for the health-status of the NP **[10]**.

Due to the lack of available data, mathematical models that have incorporated CEP permeability have used values from the cartilage literature that are typically an order of magnitude greater than that of the disc tissue **[11]**. Consequently the effect of the permeability of the CEP on fluid flow into and out of the disc would be negligible. Recently, the mechanics of a 'normal' IVD model have been compared with results from a model which had a sealed annulus or a sealed CEP **[12]**. These comparison conditions identified that the time-dependent mechanics of the IVD are notably different to 'normal' when the CEP is sealed. CEP calcification, as a consequence or a precursor to disc degeneration, may reduce the permeability of the CEP to levels similar to, or less than, that of the disc. However, the characteristics of the mechanics of a partially occluded endplate and the internal mechanics of the IVD under this condition are unknown.

This paper aims to predict the mechanical characteristics of the intervertebral disc following a reduction of the permeability of the CEPs, and to compare such a case to the previously validated **[9]** model of a 'normal' disc. Therefore, if the compression artefacts noted in the model results are seen in experimental data, then we may propose with good reason that the disc would have a reduced permeability endplate.

2 Method

The mathematical model used has been described in detail elsewhere **[9]**, and we refer the reader to this text for a full description. The model is based on that of Biot's poroelastic theory **[13]**, but with osmotic pressure, π, included in the model via the van't Hoff equation **[14]**, and strain dependent permeability of the tissue also incorporated via a power law **[15]**. The resulting system of equations reduce to the non-linear diffusion equation **[9]**:

$$\frac{\partial P^*}{\partial t} = \phi_i^2 k_i \left(P_i^*\right)^n \left(P^*\right)^2 \frac{\partial}{\partial x}\left(\frac{P^* + \dfrac{\pi_i}{\phi_i}}{\left(P^*\right)^{n+2}} \frac{\partial P^*}{\partial x} \right) \tag{1}$$

where

$$P_{(i)}^* = H_A - \frac{(1-\phi_i)}{\phi_i} P_{(i)} + \pi_i \,. \tag{2}$$

In (1) and (2), P is the fluid pore pressure, ϕ is the fluid fraction, or porosity, k is the hydraulic permeability defined in this study as the permeability of the tissue divided by the dynamic viscosity of the fluid. H_A is the aggregate modulus of the tissue under conditions of confined compression: $H_A = \dfrac{(1-\nu)}{(1+\nu)(1-2\nu)} E$, where ν and E are Poisson's ratio and Young's modulus respectively. The spatial and time dimensions are given by x and t respectively, and subscript i refers to initial conditions.

The above model is augmented by including the CEP as a varying boundary condition, by determining the pore pressure at the junction of disc and CEP by equating the fluid flux through the top of the disc with the fluid flux through a rigid porous layer representing the CEP. Then, assuming the fluid flow through the CEP obeys Darcy's law, and since the relative velocities of solid and fluid are proportional to the pressure gradients in the tissues, we have

$$\phi_b k_b \left[\phi_b \left. \frac{\partial P}{\partial x} \right|_b - \left. \frac{\partial \boldsymbol{\pi}}{\partial x} \right|_b \right] = \phi_{CEP}^2 k_{CEP} \left. \frac{\partial P}{\partial x} \right|_{CEP} \tag{3}$$

where subscripts *b* and *CEP* refer to the tissue adjacent to the CEP and the CEP itself. The pore pressure at the boundary of disc and CEP was determined for the subsequent time step by solving a discretized version of (3), which is possible since all other values, except for the pressure at the boundary of tissue and CEP, are known from the previous iteration.

Equations (1) and (2) were solved using a predictor-corrector finite difference scheme **[9]**, with equation (3) as the time-varying boundary condition, using a time step of 10 seconds. Negligible differences were found in the solution by either using a time step of 1 second, or 200 spatial nodes, or both. The parameters used to model the behavior of the disc had been previously determined by best fitting to experimental data (H_A = 4.9MPa; k_i = 9.1x10^{-16}m^4/Ns, π_i=0.1MPa) **[9]**. The CEP was assumed to be 0.6mm thick and have a constant porosity, ϕ_{CEP}, of 0.50 **[1]**, and the vertebral fluid pressure was assumed constant (0 MPa). The effect of a loss of CEP permeability on the mechanics of the IVD was predicted by using three different CEP permeabilities varying by one order of magnitude (k_{CEP} = 1x10^{-15} m^4/Ns, 5x10^{-16} m^4/Ns and 1x10^{-16} m^4/Ns) which represent the range of values quoted for articular cartilage in the literature **[16]**. The model predicted the behavior of the central section of the disc undergoing three cycles of three hours compression under a

physiologically realistic applied stress of 1MPa, followed by two hours expansion of zero applied stress.

3 Results

Figures 2, 3, and 4 show the strain, pore pressure, and relative velocity distributions for the case of the disc with (a) a CEP permeability of $1x10^{-15}$ m^4/Ns and (b) a CEP permeability of $1x10^{-16}$ m^4/Ns. In Figures 2, 3, and 4, the shading represents strain, pore pressure and relative velocity of solid and fluid respectively. The normalised height of the disc is determined from the inferior endplate (height = 0) and thus the height of the superior endplate starts from 1 and varies with time. The horizontal lines in the graphs trace the vertical position of initially equally spaced markers with respect to the inferior endplate. The mechanics using a CEP permeability of $5x10^{-16}$ m^4/Ns was very similar to that of the CEP equaling $1x10^{-15}$ m^4/Ns, and has thus not been presented.

There are clear differences in the model results when comparing condition (a) and condition (b). The loss of height with time with a reduced CEP permeability, condition (b), is nearly linear compared to the non-linear height change following a load change in condition (a). Secondly, at the end of the first 3 hours of compression, the tissue has globally strained approximately -11% in condition (a) and -8% in condition (b), showing the consequence of the loss of CEP permeability during compression. However, following the subsequent 2 hours expansion, condition (a) is now only -1.8% strained, whilst condition (b) is -4.2% strained. Therefore with a reduced permeability endplate it is evident that 2 hours of expansion are not sufficient to fully recover height lost during 3 hours of compression. This pattern is repeated over the other two cycles of compression and expansion, where after the whole 15 hour loading procedure the disc has globally strained -1.8% in case (a), but -5.5% in case (b). Thirdly, as can be seen by the shading values, the distribution of strain and pore pressure in

the disc is more homogeneous in condition (b) than (a), which result in the final observation that there lower relative velocities of solid and fluid in (b) compared to (a): maximum and minimum relative velocities of the solid and fluid are $\pm 0.15 \mu m.s^{-1}$ in case (a), but only $\pm 0.07 \mu m.s^{-1}$ in case (b).

4 Discussion

The linear change in height with time is in agreement with previous results for a completely occluded endplate **[12]**, and may be an important indicator for reduced CEP permeability. In mechanically compressing whole motion segments, it is difficult to tell a priori whether there is any disc pathology. The obvious change in deformation behavior with reduced CEP permeability may be useful in directing histological examination to the pathological site. Whilst this paper has focused on the effect of a reduced permeability CEP, it may also be the case that the same mechanics would be observed if the permeability of other spinal structures, superior and inferior to the disc, limited fluid flow into and out of the disc via the CEP. Nevertheless, the linear loss of height would indicate a pathological site out with the disc.

This study has shown that when the CEP permeability is less than that of the disc, the height change is predominantly governed by the CEP, thereby reducing the effectiveness of osmotic pressure in disc rehydration. The given loading regime resulted in a loss of height of 5.5% off the disc in the case of the reduced permeability endplate, but only 1.8% otherwise. This reduced ability to rehydrate will have obvious deleterious consequences for disc nutrition and apophyseal joint loading over a long period of time. Therefore, along with a disc with a significant loss of height associated with my may indicate a nutritional problem associated with the CEP and surrounding structiure. It has also been suggested that the CEP

also has a strain-dependent permeability **[17]** that will only add to the asymmetry of the expansion-compression mechanics and further exacerbate the problem.

The slower deformation of the IVD with a reduced CEP permeability allows time for an internal homogenization of the strain and pore pressure (and hence osmotic pressure, permeability etc) distribution. The less the pore pressure gradients the less the relative velocity of solid and fluid and thereby the internal convective transfer of solutes is reduced. This can be seen by the fact that, by reducing the permeability of the endplate by a factor of 10, the maximum and minimum relative velocities are halved. Therefore, under these conditions, the role of diffusion in the internal solute transfer becomes even more important for maintaining the healthy state of the disc. However, it must be stated that if the CEP has a low permeability, then the diffusion of solutes into the disc through the CEP is also hindered **[6]**.

It was noted in the results that the mechanics of the IVD using a CEP permeability of $5x10^{-16}$ m^4/Ns was very similar to that of the CEP equaling $1x10^{-15}$ m^4/Ns. This is the case because the model of the IVD tissue uses a strain dependent permeability. Even though the initial permeability of the solid is 9.1 $x10^{-16}$ m^4/Ns, upon application of the 1MPa load, the superior and inferior extremities strain considerably by approximately –15%. This reduces the local permeability in these extremities to a level of 2.5 $x10^{-16}$ m^4/Ns **[9]**, which is less than the permeability of the CEP, and therefore the tissue governs the mechanics. Therefore we would expect to see a transition in mechanical characteristics of the segment if the CEP permeability was less than the minimum permeability in the tissue, namely 2.5 $x10^{-16}$ m^4/Ns in this case.

The assumption of using a rigid porous layer to represent the hyaline cartilage of the CEP may affect the results: the CEP would also lose thickness and water under load possibly decreasing it's permeability further retarding the fluid flow even more. It must be stated

however, that the load imposed on the IVD is at physiological levels (1MPa), and under the dynamic strain associated with this condition, the IVD tissue has been calculated to have an aggregate modulus of 4.9MPa **[9]**. Under a similar loading scenario, bovine articular cartilage has been shown experimentally to have a dynamic unconfined modulus of approximately 23MPa at a 0.1Hz compression frequency **[18]**, which corresponds to a dynamic aggregate modulus, in confined compression, of approximately 30MPa. Therefore, since the CEP is approximately 6 times stiffer than IVD tissue, the assumption that it acts a rigid layer may be acceptable.

Disc degeneration affects the mechanical properties of the NP **[19]** and AF **[19,20]**, primarily due to the loss of PG's and water from the tissue **[21]**. Such effects have not been included in the model presented here: we have assumed that the endplate reduces in permeability whilst the disc tissue itself remains physiologically non-degenerate. Degeneration will reduce the osmotic pressure differences, lowering the disc's resistance to compression and ability to rehydrate, however, the permeability, which primarily controls the time-dependent behaviour, of degenerate disc tissue is not significantly different to 'normal' **[20]**. Therefore, if the disc tissue was degenerated then the start and end-points of compression will be different due to tissue solidification, but the time-dependent mechanics will not be greatly affected since these are controlled by the tissue's permeability. We therefore argue that the NP and AF degeneration will not have an effect on the linearisation of the deformation curve, and contribute to the reduced capacity of the disc to rehydrate.

Disc degeneration and a loss of CEP permeability have been shown to be related **[4,7]**, but whether one induces the other is still debatable. Indeed, their relation may not be causal, but it could be due to some other mechanism. On comparison with experimental data of the compression of degenerate discs **[22]** it is noticeable that no such linearisation of the height-time curve is apparent in the experimental data. Whilst this suggests that CEP

calcification does not initiate degeneration by inhibiting nutrient transfer, the opposite relation that disc degeneration may be a causal factor in CEP sclerosis, may still hold. However, such bold statements need more than one set of experimental data for verification.

5 Conclusion

This study has shown that reducing the CEP permeability below the minimum value within the disc tissue results in a greater loss of height for a given compression-expansion loading scenario, and slower movement of the fluid internally within the disc, both with possible serious consequences for disc nutrition. It has also shown that evidence for a reduction in CEP permeability may be given by a linearization of the creep loading curve and an overall loss of disc height. However, due to the lack of experimental evidence for this linearization of the height-time curve, we suggest that CEP calcification may not be the major causal factor in disc degeneration.

6 Acknowledgements

The authors would like to thank the Wellcome Trust for their generous financial support of this work (grant no. 054570/Z/98/Z).

7 References

1. **Roberts S., Menage J., and Urban J.P.G.**, Biochemical and structural properties of the cartilage end-plate and its relation to the intervertebral disc, *Spine,* 1989, **14,** 166-174.
2. **Brinkmann P., Frobin W., Hierholzer E., and Horst M.**, Deformation of the vertebral end-plate under axial loading of the spine, *Spine,* 1983, **8,** 851-856.

3. **Holmes A.D., Hukins D.W.L., and Freemont A.J.**, End-plate displacement during compression of lumbar-disc-vertebra segments and the mechanism of failure, *Spine*, 1993, **18**, 128-135.
4. **Nachemson A., Lewis T., Maroudas A., Freeman M.A.R.**, In vitro diffusion of dye through the end-plates and the annulus fibrosus of human lumbar inter-vertebral discs, *Acta Orthop. Scand.*, 1970, **41**, 589-607.
5. **Urban J.P.G., Holm S., Maroudas A., and Nachemson A.**, Nutrition of the intervertebral disc: Effect of fluid flow on solute transport, *Clin. Orthop. Relat. Res.*, 1982, **170**, 296-302.
6. **Roberts S., Urban J.P.G., Evans H, and Eisenstein S.M.**, Transport properties of the human cartilage end-plate in relation to its composition and calcification, *Spine*, 1996, **21**, 415-420.
7. **Kokkonen S.-M., Kurunlahti M., Tervonen O., Ilkko E., and Vanharanta H.**, Endplate degeneration observed on magnetic resonance imaging of the lumbar spine, *Spine*, 2002, **20**, 2274-2278.
8. **Ferguson S.J., Ito K., Nolte L.-P.**, Fluid flow paths and convective solute transport within the intervertebral disc: a computer simulation. Transactions of the 4th Annual Meeting of the Spine Society of Europe (EuroSpine), 2002, September 11-14, Nantes, France.
9. **Riches P.E., Dhillon N., Lotz J., Woods A.W., and McNally D.S.**, The internal mechanics of the intervertebral disc under cyclic loading, *J. Biomech.*, 2002, **35**, 1263-1271.
10. **Moore R.K., Osti R.L., Vernon-Roberts B., and Fraser R.D.**, Changes in end-plate vascularity after an outer anulus tear in the sheep, *Spine*, 1992, **17**, 874-878.

11. Argoubi M., and Shirazi-Adl, A., Poroelastic creep response analysis of a lumbar motion segment in compression, *J. Biomech.*, 1996, **29**, 1331-1339.

12. Ferguson S.J., Ito K., and Nolte L-P., Fluid flow and convective transport of solutes within the intervertebral disc, *J. Biomech.*, 2004, **37**, 213-221.

13. Biot M.A., General solutions of the equations of elasticity and consolidation for a porous material. *J. Appl. Mech.*, 1956, **23**, 91-6.

14. Tombs M.P., and Peacocke A.R., *The osmotic pressure of biological macromolecules*, Clarendon Press, London, 1974.

15. Koponen A, Kataja M, and Timonen J. Permeability and effective porosity of porous media. *Phys. Rev. E*, 1997, **56**, 3319-3325.

16. Reynaud B., and Quinn T.M. Anisotropic hydraulic permeability in compressed articluar cartilage. *J. Biomech.*, DOI: 10.1016/j.jbiomech.2004.10.015.

17. Ayotte D.C., Ito K., and Tepic S. Direction-dependent resistance to flow in the endplate of the intervertebral disc: an ex vivo study, *J. Orthop. Res.*, 2001, **19**, 1073-1077.

18. Park S., Hung C.T., and Ateshian G.A. Mechanical response of bovine articular cartilage under dynamic unconfined compression loading at physiological stress levels. *Osteoarthr. Cartilage*, 2004, **12**, 65-73.

19. Umehara S., Tadano S., Abumi K., Katagiri K., Kaneda K., Ukai, T., Effects of degeneration on the elastic modulus distribution in the lumbar intervertebral disc, *Spine*, **21**, 811-820.

20. Iatridis J.C., Setton L.A., Foster R.J., Rawlins B.A., Weidenbaum M., and Mow V.C., Degeneration affects the anisotropic and nonlinear behaviors of human anulus fibrosus in compression, *J. Biomech.*, 1998, **31**, 535-544.

21. **Urban J.P.G. and McMullin J.F.**, Swelling pressure of the lumbar intervertebral discs: influence of age, spinal level, composition and degeneration, *Spine*, 1988, **13**, 179-187.

22. **Dhillon N, Bass E.C., and Lotz J.C.**, Effect of frozen storage on the creep behavior of human intervertebral discs, *Spine*, 2001, **26**, 883-888.

8 Figures

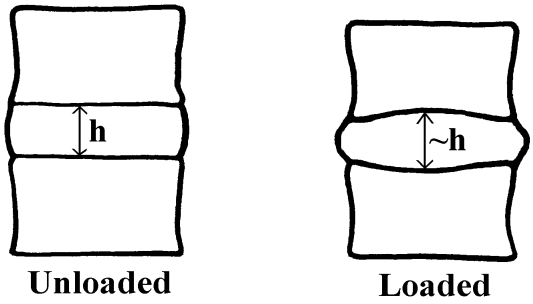

Figure 1: Schematic diagram of the deformation of a motion segment under axial compression (h = height of unloaded disc).

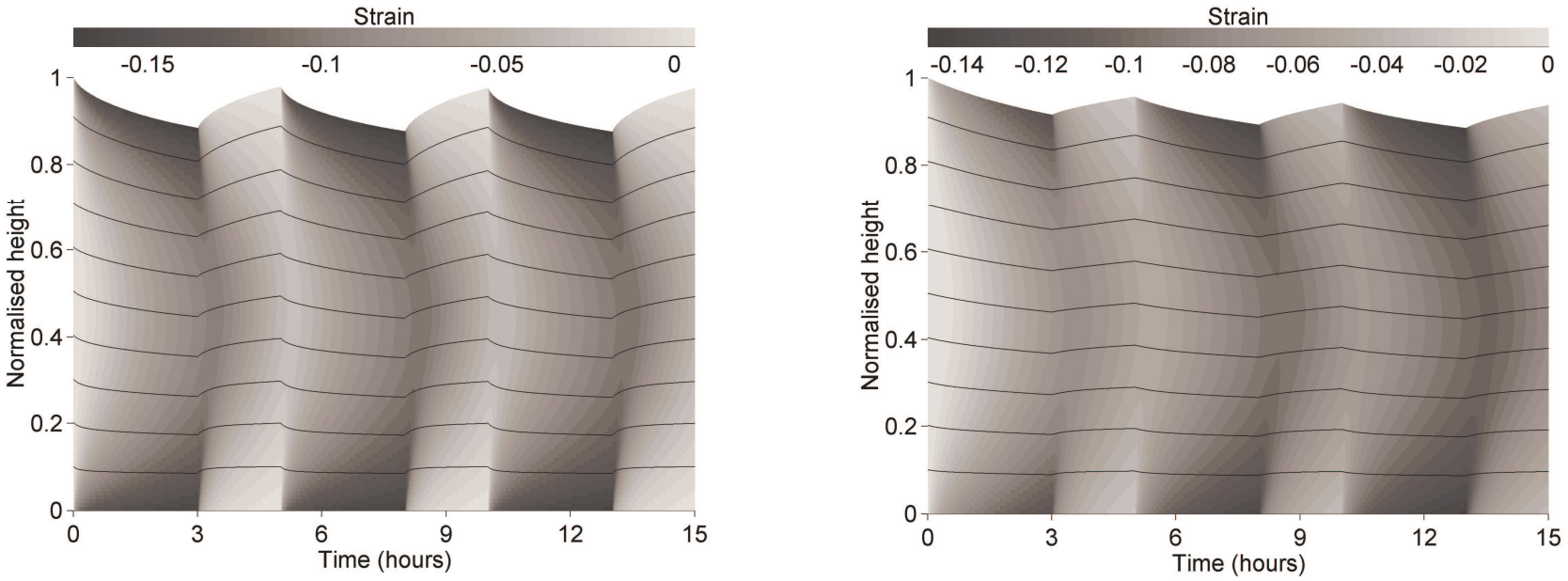

(a) (b)

Figure 2: Strain distribution in the IVD with (a) k_{CEP} = 1x10^{-15} m^4/Ns and (b) k_{CEP} = 1x10^{-16} m^4/Ns

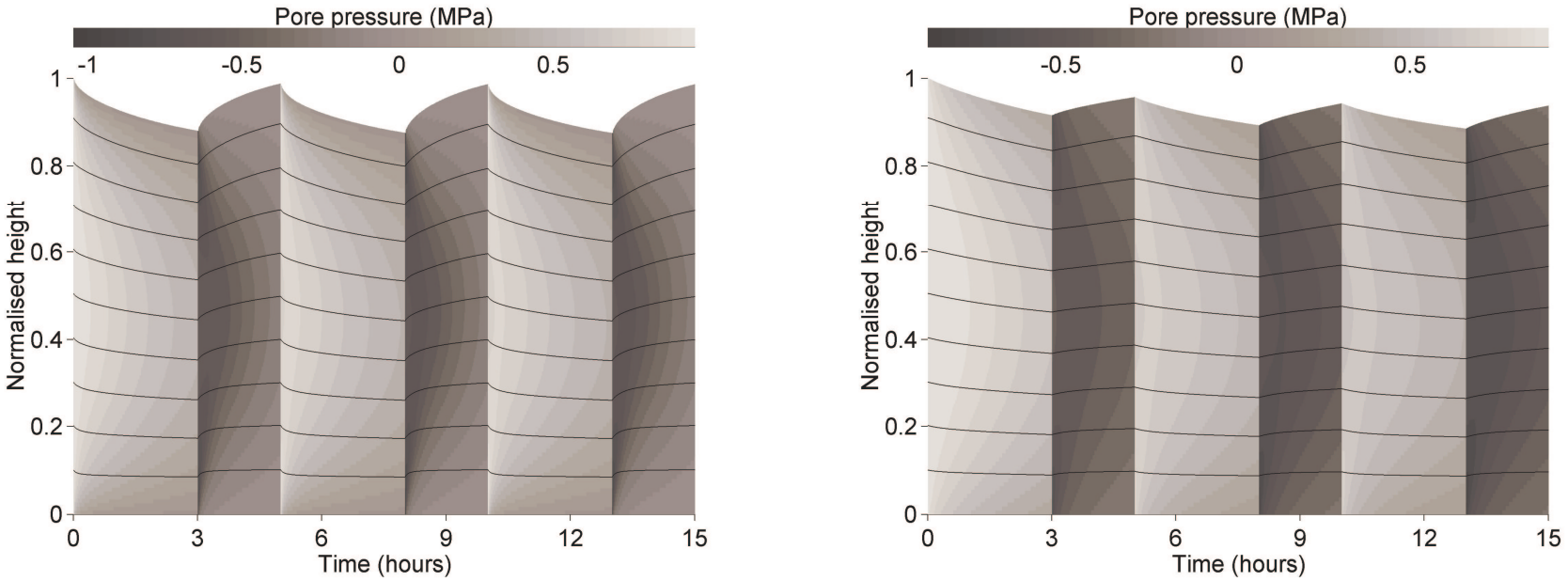

(a) (b)

Figure 3: Pore pressure distribution in the IVD with (a) k_{CEP} = 1x10^{-15} m^4/Ns and (b) k_{CEP} = 1x10^{-16} m^4/Ns

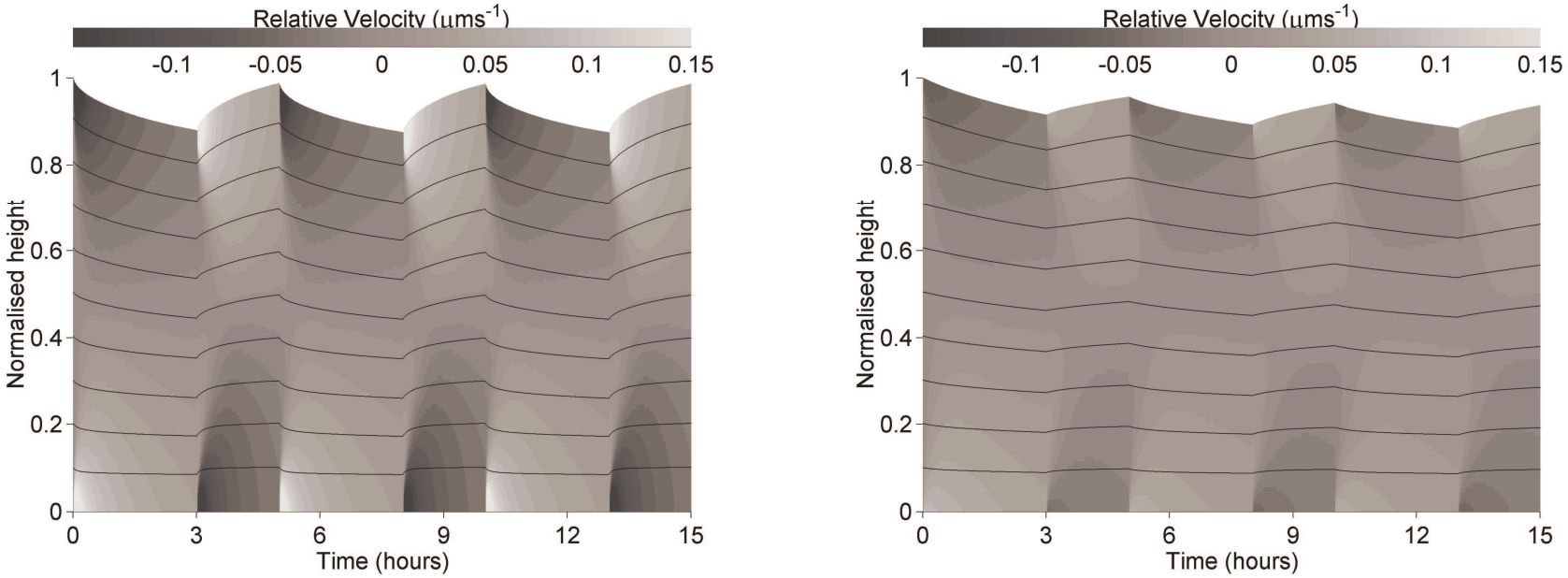

(a) (b)

Figure 4: Relative velocity distribution in the IVD with (a) k_{CEP} = 1x10^{-15} m^4/Ns and (b) k_{CEP} = 1x10^{-16} m^4/Ns

9 Figure Captions

Figure 1: Schematic diagram of the deformation of a motion segment under axial compression (h = height of unloaded disc).

Figure 2: Strain distribution in the IVD with (a) $k_{CEP} = 1x10^{-15}$ m^4/Ns and (b) $k_{CEP} = 1x10^{-16}$ m^4/Ns

Figure 3: Pore pressure distribution in the IVD with (a) $k_{CEP} = 1x10^{-15}$ m^4/Ns and (b) $k_{CEP} = 1x10^{-16}$ m^4/Ns

Figure 4: Relative velocity distribution in the IVD with (a) $k_{CEP} = 1x10^{-15}$ m^4/Ns and (b) $k_{CEP} = 1x10^{-16}$ m^4/Ns